Biochimica et Biophysica Acta 1788 (2009) 1310–1320

Contents lists available at ScienceDirect

Biochimica et Biophysica Acta

journal homepage: www.elsevier.com/locate/bbamem

Thermotropic behavior and lateral distribution of very long chain sphingolipids

Y. Jenny E. Björkqvist [a], Jonathan Brewer [b], Luis A. Bagatolli [b], J. Peter Slotte [a], Bodil Westerlund [a,*,1]

[a] Department of Biochemistry and Pharmacy, Åbo Akademi University, Turku, Finland
[b] Membrane Biophysics and Biophotonics group/MEMPHYS Center for Biomembrane Physics, Department of Biochemistry and Molecular Biology, University of Southern Denmark, Odense, Denmark

ARTICLE INFO

Article history:
Received 5 December 2008
Received in revised form 25 February 2009
Accepted 26 February 2009
Available online 9 March 2009

Keywords:
Cholesterol
Galactosylceramide
Glucosylceramide
Sphingomyelin
Differential scanning calorimetry
Fluorescence spectroscopy

ABSTRACT

Sphingolipids containing very long acyl chains are abundant in certain specialized tissues and minor components of plasma membranes in most mammalian cells. There are cellular processes in which these sphingolipids are required, and the function seems to be mediated through sphingolipid-rich membrane domains. This study was conducted to explore how very long acyl chains of sphingolipids influence their lateral distribution in membranes. Differential scanning calorimetry showed that 24:0- and 24:1-sphingomyelins, galactosylceramides and glucosylceramides exhibited complex thermotropic behavior and partial miscibility with palmitoyl sphingomyelin. The T_m was decreased by about 20 °C for all 24:1-sphingolipids compared to the corresponding 24:0-sphingolipids. The ability to pack tightly with ordered and extended acyl chains is a necessity for membrane lipids to partition into ordered domains in membranes and thus the 24:1-sphingolipids appeared less likely to do so. Fluorescence quenching measurements showed that the 24:0-sphingolipids formed ordered domains in multicomponent membranes, both as the only sphingolipid and mixed with palmitoyl sphingomyelin. These domains had a high packing density which appeared to hinder the partitioning of sterols into them, as reported by the fluorescent cholesterol analog cholestatrienol. 24:0-SM was, however, better able to accommodate sterol than the glycosphingolipids. The 24:1-sphingolipids could, depending on head group structure, either stabilize or disrupt ordered sphingolipid/cholesterol domains. We conclude that very long chain sphingolipids, when present in biological membranes, may affect the physical properties of or the distribution of sterols between lateral domains. It was also evident that not only the very long acyl chain but also the specific molecular structure of the sphingolipids was of importance for their membrane properties.

1. Introduction

The sphingolipids (SLs) are major components of the external leaflet of plasma membranes in most mammalian cells. Natural SLs display an extensive structural diversity in the hydrophilic head group, consisting either of a phosphorylcholine group (in sphingomyelin; SM) or one or several carbohydrate residues (in glycosphingolipids; GSLs). The wide variety in head group structures among GSLs found in biological systems seems to reflect their function as recognition sites at the cell surface. Several GSLs have been identified as targets for different pathogens which attach and internalize through specific GSL-enriched membrane regions [1]. The GSLs in the plasma membrane are also involved in cell adhesion and signaling, by communicating with the cell environment through their sugar head groups or by laterally affecting the activity and location of growth factors and signal transducers within the same membrane [2,3].

The ceramide structure of natural SLs varies mainly with respect to the acyl chain, which usually is 16–26 carbons long, mostly saturated and amide-linked to the 18–20 carbons long sphingoid base. SLs containing very long acyl chains (usually defined as >20 carbons [4]) occur in large amounts in certain specialized tissues, such as brain, retina and skin, and are minor components of plasma membranes in other cell types. There is evidence of cellular processes in which the presence of SLs with very long acyl chains is indispensable [5,6]. However, many characterized functions of SLs have been ascribed to head group specific lipids, although the hydrophobic part of the molecules seems to have a large impact on their biological function. It has been shown that a long ceramide unit, as compared to the surrounding lipids, may increase the binding efficiency of ligands to GSLs at the membrane surface [7,8]. Since the orientation of the sugar head group still seems to be unaffected by modifications in the ceramide structure [9,10], the

Abbreviations: 7SLPC, 1-palmitoyl-2-stearoyl-(7-doxyl)-*sn*-glycero-3-phosphocholine; CTL, cholestatrienol; DPH, diphenylhexatriene; GalCer, galactosylceramide; GlcCer, glucosylceramide; GSL, glycosphingolipid; GUV, giant unilamellar vesicle; POPC, 1-palmitoyl-2-oleoyl-*sn*-glycero-3-phosphocholine; PSM, D-*erythro*-*N*-palmitoyl-sphingomyelin; SL, sphingolipid; SM, sphingomyelin; T_m, gel-to-liquid phase transition temperature; tPA, *trans*-parinaric acid; VLC, very long chain

* Corresponding author. Tel.: +358 2 2154816; fax: +358 2 2154745.
E-mail address: bodil.westerlund@abo.fi (B. Westerlund).
[1] Formerly Ramstedt.

0005-2736/$ – see front matter © 2009 Elsevier B.V. All rights reserved.
doi:10.1016/j.bbamem.2009.02.019

improved receptor ability was explained to originate in the motional properties of the hydrophobic part of the bilayer which are influenced by the acyl chain length [9,11].

The lateral elasticity and phase transitions of acyl chain defined SLs have been thoroughly characterized with monolayer techniques by Brown and coworkers [12–14]. These studies have shown that GSLs in general display a lower in plane elasticity, i.e. a higher lateral packing, than chain matched SMs [12–14]. Concerning SLs with very long acyl chains, it is however of great importance to consider the effects of both bilayer leaflets when evaluating their membrane behavior. The very long acyl chain provides the SL molecule with a chain length asymmetry at the bilayer midplane, where the acyl chain may extend into the opposing bilayer leaflet. Such interdigitation has been described for C24 SM [15,16] and appears to apply to several neutral and charged long chain GSLs with different degrees of head group complexity [17,18]. Recent molecular dynamics simulations on SM bilayers show that interdigitation is slightly more pronounced in monounsaturated SMs than in saturated ones, in which the terminal part of the long acyl chain instead may bend before the center of the bilayer [19]. Scanning calorimetric studies on various long chain GSLs have revealed complex mesomorphic phase behavior characterized by irreversible transitions between different stable and metastable gel phases and very high chain-melting temperatures [20–23].

As expected from their high gel-to-liquid phase transition temperatures (T_m), GSLs tend to segregate from low T_m phospholipids in mixed membranes [24,25]. The GSL-enriched domains have a tight lateral packing density due to stabilizing hydrogen bond networks formed between adjacent carbohydrate groups and the surrounding water, and hydrophobic interactions between the highly saturated hydrocarbon chains [26]. The dense lipid packing seems to make cholesterol less miscible with GSLs compared to chain matched SMs at temperatures below the T_m of the SL. However, many GSLs partition readily into ordered domains composed of SMs and cholesterol [27,28]. The miscibility of cholesterol with GSLs is furthermore influenced by the head group structure, and we have previously shown that a change in the stereochemical orientation of one hydroxyl group in the sugar molecule makes cholesterol more prone to interact with glucosylceramide (GlcCer) than galactosylceramide (GalCer) [27]. In addition, the partitioning of cholesterol between GSL-rich domains and a fluid phospholipid rich environment may depend on the properties of the low T_m phospholipid [29].

Previous studies suggest that various ordered domains coexist independently in biological membranes and that the domains differ in SL and protein content [30–32]. The composition of membrane domains may also change upon external stimulation or at specific physiological or pathological conditions. SMs and GlcCers containing C24:1 acyl chains have for instance been observed at elevated concentrations in detergent-insoluble GSL-rich domains in multidrug resistant cancer cells as compared to drug sensitive cells [33]. It appears likely that the physical and functional properties of different membrane domains are affected by their SL composition. However, information about how different structural aspects of the SLs affect their partitioning between different domains is still limited.

This study was conducted to investigate the effect of a very long saturated (24:0) or monounsaturated ($24:1^{\Delta cis15}$) acyl chain on the lateral membrane distribution of SLs with relatively simple head groups. The tendency of C24 SMs, GalCers and GlcCers to phase separate and form lateral SL-enriched domains in phospholipid/cholesterol bilayers was explored using a fluorescence quenching assay. In addition, we studied the ability of the very long chain SLs to mix with and co-cluster with palmitoyl-SM which from previous studies is known to form ordered lateral domains with cholesterol. The results are discussed in comparison to our previous data on the corresponding SLs containing 16:0 acyl chains.

2. Materials and methods

2.1. Materials

Lyso-GalCer (D-galactosyl-β1-1′-D-*erythro*-sphingosine), lyso-GlcCer (D-glucosyl-β1-1′-D-*erythro*-sphingosine) and lyso-SM (D-*erythro*-sphingosylphosphorylcholine) for synthesis of the very long chain sphingolipids (VLC-SLs) were obtained from Avanti Polar Lipids (Alabaster, AL), lignoceric acid (24:0) from Sigma Chemicals (St. Louis, MO) and nervonic acid ($24:1^{\Delta cis15}$) from Larodan Fine Chemicals (Malmö, Sweden). The VLC-SLs were synthesized from the corresponding lyso-derivatives and fatty acids according to a modified version of the method for SM synthesis originally published by Cohen et al. [34]. In brief, the lyso-derivative (lyso-galactosylceramide, lyso-glucosylceramide or lyso-sphingomyelin) and the fatty acid (lyso-sphingolipid/fatty acid, 1:10 molar ratio) were dissolved in dichloromethane/methanol (11:1, vol:vol) containing 1 vol.% triethylamine. N,N′-dicyclohexylcarbodiimide (DCC; Fluka, Buchs, Switzerland) was added as a catalyst (DCC/fatty acid, 1.2:1, molar ratio) and the reactions were carried out at 35 °C (24:0-SLs) or at room temperature (24:1-SLs) for 16 h. The VLC-SLs were purified by reverse-phase HPLC on a preparative Supelco Discovery C18 column (250 × 21.2 mm, 5 μm particle size) with methanol as eluent. The purity and identity of the products were verified with HPTLC and the molecular ions verified by MS analysis (Micromass Quattro II mass spectrometer, Manchester, UK).We have previously successfully used this method for sphingolipid synthesis and product verification in several studies [27,35–38].

D-*erythro*-*N*-palmitoyl-sphingomyelin (PSM) was purified from egg yolk SM (Avanti Polar Lipids) as previously described [27]. 1-Palmitoyl-2-oleoyl-*sn*-glycero-3-phosphocholine (POPC) was obtained from Avanti Polar Lipids and cholesterol from Sigma Chemicals. (7-Doxyl)-stearic acid (TCI Europe N.V., Belgium) and lyso-phosphatidylcholine (1-palmitoyl-2-OH-*sn*-glycero-3-phosphocholine; Avanti Polar Lipids) were used for the synthesis of 1-palmitoyl-2-stearoyl-(7-doxyl)-*sn*-glycero-3-phosphocholine (7SLPC) according to the method described by Szolderits et al. [39]. Stock solutions of the lipids were prepared in hexane/isopropanol, 3:2, vol:vol (phospholipids and cholesterol) or in chloroform/methanol, 2:1, vol:vol (GSLs), stored in the dark at −20 °C and warmed to ambient temperature before use.

Cholestatrienol (cholesta-5,7,9(11)-trien-3-beta-ol; CTL) was synthesized according to Fischer et al. [40] and purified by reverse-phase HPLC with acetonitrile/methanol (7:3, vol:vol) as the eluent. *trans*-Parinaric acid (tPA) was produced by isomerization of *cis*-parinaric acid (Cayman Chemical Company, Ann Arbor, MI) as described by Sklar et al. [41] and purified by reverse-phase HPLC using methanol/water/acetic acid (900:50:3, vol:vol) as the eluent. The synthesized fluorescent probes were stored dry under argon in the dark at −87 °C until solubilized in argon-purged ethanol (CTL) or methanol (tPA). Stock solutions of the CTL and tPA were stored in the dark at −20 °C and used within five days. Stock solutions of 1,1′-dioctadecyl-3,3,3′,3′-tetramethylindocarbocyanine perchlorate (DiI_{C18}) and 1,6-diphenyl-1,3,5-hexatriene (DPH), both from Molecular Probes (Invitrogen, Copenhagen, Denmark or Eugene, OR), were prepared in methanol and stored in −20 °C.

The water used was purified by reverse osmosis followed by passage through a Millipore UF Plus water purification system, to yield a product with a resistivity of 18.2 MΩcm. The water was additionally argon-saturated before being used for samples containing tPA or CTL to minimize the risk of probe oxidation.

2.2. Sample preparation

The appropriate amounts of lipids (and fluorescent probes) were mixed and the solvent was evaporated under a stream of nitrogen and under high vacuum. The multicomponent samples used in

fluorescence quenching experiments were additionally redissolved and thoroughly mixed in chloroform before being kept in vacuum. The dry lipid films were hydrated in warm water (70–90 °C for pure SL and SL/PSM samples or 60 °C for more complex lipid mixtures), briefly vortexed and then sonicated. DSC samples were bath sonicated for 20 min at 70–90 °C in a Branson bath sonicator 2510 (Branson Ultrasonics, Danbury, CT) whereas fluorescence samples were probe sonicated for 2 min at 60 °C (25% duty cycle, power output 10 W) with a Branson probe sonifier W-450 (Branson Ultrasonics). The final lipid concentrations of the samples were 2 mM (DSC) or 50 μM (fluorescence experiments).

Giant unilamellar vesicles (GUVs) were produced as previously described [42] by the electroformation method originally described by Angelova et al. [43]. The vesicles were composed of POPC: SL: cholesterol (60:30:10, molar ratio) and labeled with DiI_{C18} at 0.5 mol%. The lipid mixtures (0.2 mg/ml in chloroform/methanol, 2:1, vol:vol) containing the fluorescent probe were deposited on cylindrical Pt electrodes in special chambers designed for GUV preparation (3 μl of lipid solution on each electrode). The solvent was evaporated under high vacuum over night. The chamber was then coupled to a circulating water bath (75 °C), 300 μl of sucrose solution (200 mOsm) was added and a low frequency AC field was applied (Vann Draper Digimess Fg 100, Stenson, Derby, UK; sine function, freq. 10 Hz, amplitude 2.0 V). After 1 h of electroformation, the frequency was lowered to 1.0 Hz to allow the vesicles to diffuse from the electrodes. The vesicles (in sucrose) were transferred to an iso-

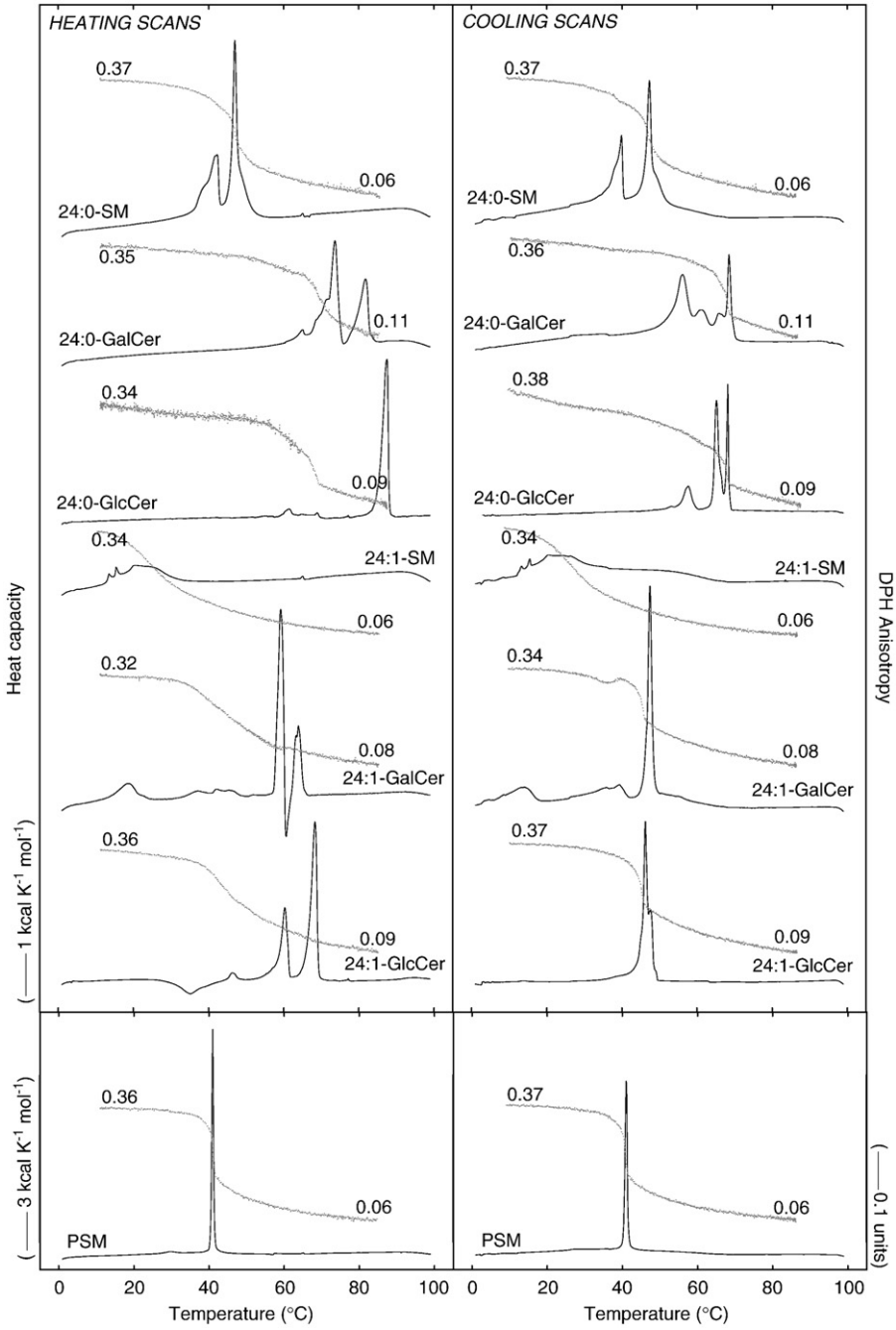

Fig. 1. Thermotropic behavior of all the SLs used in the study. DSC samples were prepared of 100% PSM or VLC-SLs at a lipid concentration of 2 mM, and representative heating and cooling scans obtained after sample equilibration are shown (black solid lines). DPH anisotropy was determined in the corresponding SL bilayers (DPH added at 0.5 mol%) prepared at a lipid concentration of 50 μM (superimposed grey dotted lines). The DPH anisotropy values at 12 °C and 84 °C are indicated at the ends of the traces. The scan rates were 0.5 °C/min (DSC) and 2 °C/min (DPH anisotropy).

osmolaric glucose solution in a microscope chamber (LabTek, Naperville, IL) whereby the vesicles (of higher density) sank to the bottom of the chamber and were ready for observation with an inverted microscope.

2.3. Differential scanning calorimetric measurements

DSC samples were composed of 100% VLC-SL or PSM: VLC-SL (1:1, molar ratio). DSC measurements were performed in a Calorimetry Sciences Corporation Nano II DSC (Provo, UT). The samples were loaded into the calorimeter and subjected to at least three consecutive heating and cooling scans between 0 and 100 °C at a rate of 0.5 °C/min. We observed the repeated heating (and cooling) thermograms to be essentially identical in shape and heat capacity after 2–4 heating/cooling cycles with this scan rate, and all DSC data shown represent the scan appearance after sample equilibration.

2.4. Steady-state fluorescence experiments

Fluorescence measurements were performed on a PTI Quanta-Master spectrofluorimeter operating in the T- (or L-) format (Photon Technology International, Lawrenceville, NJ). The measurements were performed in quartz cuvettes and the sample solutions were kept at constant stirring throughout the measurements. The temperature was controlled by a Peltier element, with a temperature probe immersed in the sample solution. The excitation and emission slits were set to 5 nm and the wavelengths were adjusted with monochromators (or dichroic and bandpass filters). The excitation/emission wavelengths used were 358 nm/430 nm for DPH, 324 nm/374 nm (or 321 ± 5 nm/>385 nm) for CTL and 305 nm/410 nm (or 310 ± 5 nm/>420 nm) for tPA.

2.4.1. DPH anisotropy measurements

Samples for DPH anisotropy experiments were composed of 100% VLC-SL or PSM: VLC-SL (1:1, molar ratio) with DPH added at 0.5 mol%. The G factor was determined at 10 °C prior to each measurement and the samples were then scanned at a rate of 2 °C/min.

2.4.2. Fluorescence quenching measurements

A fluorescence quenching method (described in detail in previous publications [44,45]) was applied to detect coexistence of ordered and disordered domains in multicomponent membranes. Briefly, the samples used were composed of POPC: SLs: cholesterol (60:30:10, molar ratio; F_0 samples) or POPC: 7SLPC: SLs: cholesterol (30:30:30:10, molar ratio; F samples) with the fluorescent probe (CTL or tPA) added at 1 mol%. The samples were scanned at a rate of 5 °C/min during the measurements. The fluorescence intensity of quencher containing F samples was then compared to the fluorescence intensity of quencher free F_0 samples, giving the fraction of unquenched fluorescence (F/F_0). The formation of ordered domains by the SLs (and cholesterol) was detected with tPA as a marker for all ordered domains or with CTL as a specific marker for ordered sterol-enriched domains [27]. 7SLPC was included as a quenching lipid that associates predominantly with the disordered POPC rich domains (Halling, K.K, Westerlund, B. and Slotte, J.P., unpublished calorimetric data). The fluorescent probes will therefore be protected from quenching when localized in ordered domains, and the fluorescence intensity (F/F_0) gives a measure on the extent of ordered domains formed in the membrane. A decrease in fluorescence intensity (i.e. increase in quenching) observed as the bilayer is heated indicates when the ordered domains dissociate. The thermostability of the ordered domains in different systems can be measured by looking at the quenching susceptibility of the probe as a function of temperature. The changes in quenching are reversible in bilayers containing PSM as the domain building lipid after temperature scans to at least 80 °C (results not shown) indicating probe and quencher stability throughout the experiments. The fluorescent probes were protected from light during all steps and solvents were saturated with argon before use in order to minimize the risk of oxidation.

2.5. Determination of transition temperatures

The transition temperatures were determined from the DSC and DPH anisotropy data using the Origin7 software. The derivative of the DPH anisotropy scans was analyzed to give the mid temperatures of the transition intervals. Several transition temperatures are given in the cases were several transition intervals were identified by the software.

2.6. Fluorescence microscopy experiments

An inverted Zeiss-LSM 510 META NLO microscope (Zeiss, Jena, Germany) was used for imaging of DiI_{C18} labeled GUVs. The excitation wavelength was 543 nm and the fluorescence signal was collected using a bandpass filter of 590 ± 25 nm. The objective used was a 40× water immersion with numerical aperture 1.2.

3. Results and discussion

3.1. Thermotropic behavior of the VLC-SLs

DSC was applied to analyze the thermotropic properties of the pure SLs. Fig. 1 shows representative thermograms of the VLC-SLs and PSM recorded in the heating and cooling modes with a scan rate of 0.5 °C/min (black solid lines). All the VLC-SLs displayed very complex thermotropic behavior with several phase transitions observed in both scanning directions. All the phase transitions (T_1–T_4) detected for SLs upon heating are summarized in Table 1. The method used does not allow identification of the different lipid phases, but previous combined DSC and X-ray diffraction studies have attributed the peaks at lower temperature (T_1–T_3 in Table 1) to conversions between different metastable gel phases, which differ in the hydrocarbon packing mode, chain tilt, degree of chain interdigitation and hydration of the head group [22,46]. The metastable phases are strongly affected by the scan rate, hydration level and possible pre-incubation of the sample and thus vary heavily between different studies [22,46,47]. The shape of the thermograms in Fig. 1 agreed well with previously reported data for 24:1-GalCer [21,47], 24:1-SM [21], 24:0-GalCer [22] and 24:0-SM [46,48], although the peaks were slightly shifted in temperature especially in the case of the 24:0 species. The highest temperature transition of the heating scan (T_4 in Table 1), which according to previous studies corresponds to the chain-melting transition from gel or lamellar crystalline phase to liquid-crystalline

Table 1
Transition temperatures (T_n) of VLC-SLs and PSM according to DSC and DPH anisotropy heating data.

	DSC				DPH anisotropy		
	T_1	T_2	T_3	T_4	T_I	T_{II}	T_{III}
24:0-SM			42	47	42	47	
24:0-GalCer		65	74	82	59 ± 1	71 ± 1	
24:0-GlcCer			61	88	61	68	
24:1-SM		14	16	23 ± 3		24 ± 1	
24:1-GalCer	19	59	(−)61	64		43 ± 1	(−)60
24:1-GlcCer	(−)35	46	60	68		45 ± 1	
PSM			30	41		41	

The highest temperature peak of the DSC scan (T_4) corresponds to the transition from gel or crystalline phase to liquid-crystalline phase (T_m), whereas the peaks at lower temperatures (T_1–T_3) represent transitions between different metastable phases. The DSC scan rate was 0.5 °C/min. The transitions derived from the DPH anisotropy data are labeled T_I–T_{III}. A peak corresponding to T_4 was only detected for the SMs with DPH anisotropy at a scan rate of 2 °C/min (T_{II}). The negative sign indicates exothermic transitions. The variation in temperature was less than ± 1 °C unless otherwise stated.

phase, appears less dependent on the above-mentioned parameters [22,46]. The chain-melting temperatures (T_m) detected for the VLC-SLs were in fairly good agreement with previous findings where such were available [21,22,46,47,49]. Any DSC data on the acyl chain specific VLC-GlcCers has not, to the best of our knowledge, been published previously but the detected T_m for 24:0-GlcCer was similar to that reported for a 16:0-GlcCer (87 °C) [50]. The introduction of a *cis* double bond in the acyl chain lowered the T_m of the 24:1-SLs by ~20 °C compared to the corresponding saturated ones. Nevertheless, also the unsaturated GalCer and GlcCer exhibited very high T_m's, well above physiological temperature. Extensive hydrogen bonding networks in the carbohydrate head group region is likely to account for the higher T_m's observed for all the VLC-GSLs compared to the VLC-SMs [26].

Since the thermotropic properties of many GSLs have been shown to be polymorphic and largely dependent on the sample history it is difficult to compare results from different studies. We therefore recorded DSC data on all SLs used in this study and treated all samples equally to obtain comparable results. One should however be aware that the different lipids might react differently to scan rates and sample history, which limits the interpretation of the absolute results. Galactolipids have previously also been shown to sometimes occur in lamellar crystalline (Lc) phase, which differs from gel phases in having slower transition kinetics [51]. The most stable phases seen here for the GSLs might have been Lc-phases making the results even more susceptible to the scanning rate. The GalCer and GlcCer traces were also significantly different in the heating mode as compared to the cooling mode. Such hysteresis was less pronounced for the SMs. The DSC data of PSM is also shown since this SL was used as a reference lipid throughout the study. PSM experienced a highly cooperative and reversible transition at 41 °C in agreement with previous reports [52,53].

The membrane properties of the VLC-SLs were further investigated by measuring the anisotropy of DPH in the corresponding SL bilayers (Fig. 1, grey dotted lines). DPH partitions predominantly into the hydrophobic core of lipid bilayers, with a nearly equal affinity for all lipid phases [54]. The anisotropy of DPH is sensitive to changes in the lipid chain order. In the saturated SM samples (PSM and 24:0-SM), DPH detected a sharp decrease in the chain order at the high-temperature chain-melting transitions (41 °C and 47 °C, respectively) observed with DSC upon heating (Fig 1 and Table 1). The low temperature transition of the 24:0-SM sample (around 41 °C) was also

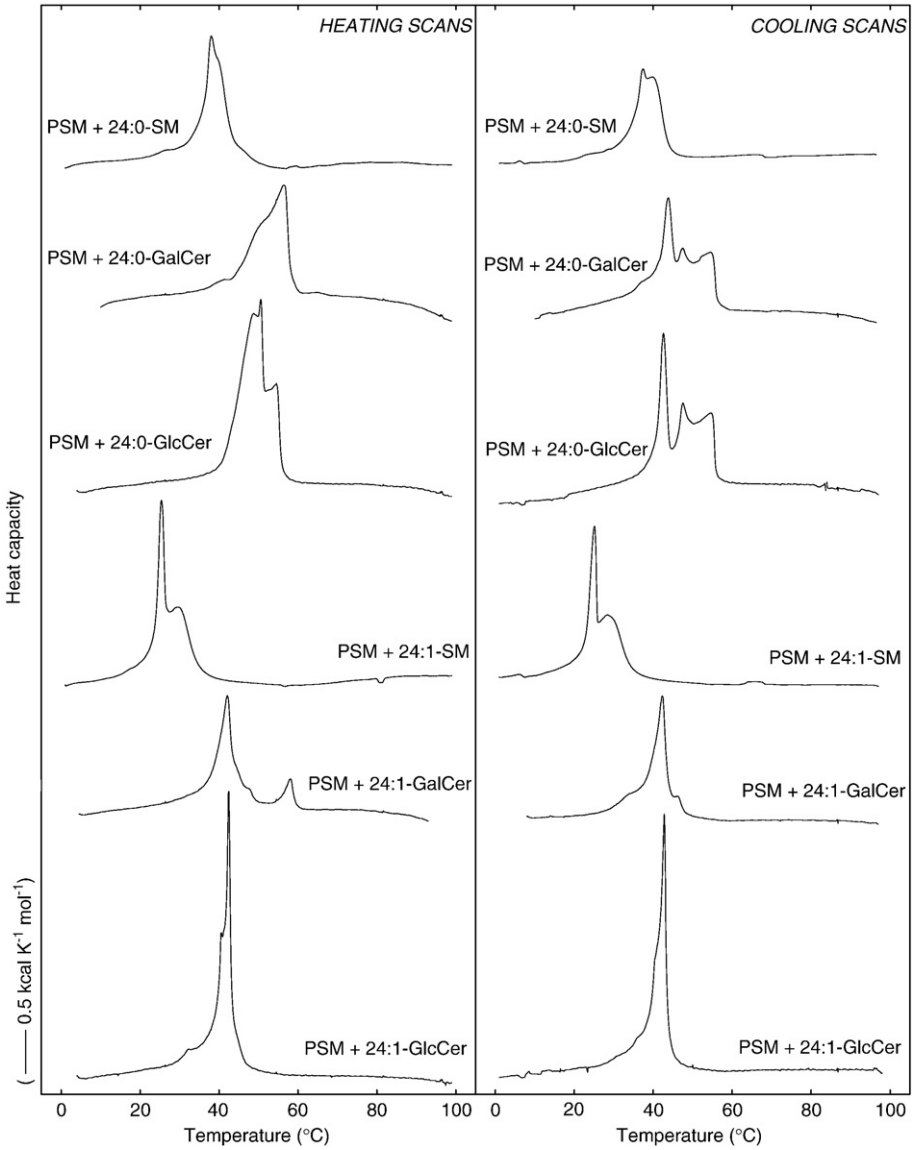

Fig. 2. Representative DSC scans of equimolar mixtures of PSM and VLC-SLs. Heating and cooling scans obtained after sample equilibration are shown. The lipid concentration was 2 mM and the scan rate used was 0.5 °C/min.

detected by DPH but did not affect the lateral lipid order significantly. The T_m of 24:1-SM was also similarly reported by DSC and DPH anisotropy measurements but the transition was less cooperative in the case of this unsaturated SM.

Concerning the VLC-GSLs, it is obvious from the DPH anisotropy data that the membrane order was drastically reduced already at temperatures below their T_m, which suggests that DPH was sensitive to conversions between different metastable gel phases. The DPH anisotropy decreased at broader temperature intervals in the 24:0-GSL bilayers as compared to the saturated SM bilayers, and the decrease did not coincide with the highest temperature transition of the 24:0-GSLs observed in the DSC heating scans. This might be due to the different heating rate in the anisotropy measurements, which might have been too fast for the lipids to convert into more stable phases. It is also possible that the decrease in DPH anisotropy in these samples was caused by transitions to temporary metastable liquid-crystalline phases existing below the T_m, as has been documented for 24:0-GalCer [22]. Reed and Shipley presented a model for the phase transitions of 24:0-GalCer bilayers where a metastable gel phase converts to a metastable liquid-crystalline phase upon heating through 69 °C, the latter subsequently converting to a more stable crystal phase at 72 °C which in turn undergoes the chain-melting transition at 82 °C [22]. In our 24:0-GalCer system, DPH displayed a large decrease in lipid chain order at 71 ± 1 °C but was unable to detect any phase transitions above this temperature. The DPH probe might also be excluded from highly ordered crystal phases and therefore be unable to report on the melting of such phases. The 24:1-SLs displayed even more gradual declines in DPH anisotropy with increasing temperature. Upon cooling, DPH reported on very cooperative liquid-crystalline to (metastable) gel phase transitions in all samples, in good agreement with the high-temperature peaks reported by DSC. However, from the cooling data it appears that DPH in most cases was insensitive to the conversions between different metastable gel phases upon further cooling, which is possible if these for instance only involved the sugar head groups and thus did not affect the DPH molecule in the hydrophobic core of the bilayer. The transition temperatures (T_I–T_{III}) detected from the DPH anisotropy data are also summarized in Table 1. These were taken as the midpoints of each transition interval as described in the Methods section.

3.2. Miscibility of the VLC-SLs with PSM

DSC was also employed to study the miscibility of the VLC-SLs with PSM, which is the dominant SM species in most mammalian cells. Fig. 2 shows the calorimetric data for equimolar binary mixtures of VLC-SLs and PSM. The results recorded in the heating mode suggest that none of the VLC-SLs mixed ideally with PSM since all thermograms consisted of at least two components. However, the transitions of the pure SLs (VLC-SL or PSM) were not observed in most of the thermograms, indicating that the two lipid components were at least partially mixed. The PSM/VLC-SM mixtures showed essentially identical thermotropic behavior independent on the scanning direction, in accordance with the DSC data of the pure SMs.

The peak maximum and peak widths at half-height of the detected transitions are presented in Table 2. All the binary mixtures displayed relatively high melting temperatures, except for PSM/24:1-SM. According to the relatively narrow peak widths (Table 2) 24:0-SM seemed to mix fairly well with PSM, which was expected considering the identical head groups. However, DSC was not a good method for determining their miscibility due to the quite similar T_m of the pure lipids (47 °C and 41 °C, respectively). More surprising was the good miscibility of 24:1-GlcCer and PSM also deduced from the narrow peak width. The nearly reversible thermotropic behavior of the PSM/24:1-GlcCer mixture is also an indication of good intercalation of PSM with the 24:1-GlcCer molecules. It has previously been shown that the

Table 2
Peak maximum (T_{max}) and peak widths at half-height ($\Delta T_{1/2}$) of transitions in binary mixtures of PSM + VLC-SL[a] and PSM according to DSC heating data scanned from 0 to 100 °C at a rate of 0.5 °C/min.

	DSC	
	T_{max} (°C)	$\Delta T_{1/2}$ (°C)
PSM + 24:0-SM	38	~5
PSM + 24:0-GalCer	56	~10
PSM + 24:0-GlcCer	51	~10
PSM + 24:1-SM	25	~7
PSM + 24:1-GalCer	42, 58	~5, ~2
PSM + 24:1-GlcCer	42	~3
PSM	41	~0.5

[a] 1:1, molar ratio.

presence of 15% dipalmitoyl-phosphatidylcholine (DPPC), which has a similar T_m as PSM (~41 °C [55]), eliminated the hysteresis of a natural GlcCer mixture from Gaucher's spleen [56]. The DPPC molecules were suggested to intercalate between the GlcCer molecules in the liquid-crystalline phase and thereby prevent their transition from metastable to stable gel phase upon cooling. According to our results, 50% PSM hindered the native hysteretic behavior of 24:1-GlcCer, but not that of 24:0-GalCer, 24:1-GalCer and 24:0-GlcCer. This indicates that some fractions of the latter three VLC-SLs existed in segregated, relatively PSM poor domains. A peak that presumably originated from the melting of almost pure 24:1-GalCer was indeed discernible in the PSM/24:1-GalCer heating scan (at ~58 °C). We have previously shown that 16:0-GalCer is completely miscible with PSM when mixed 1:1 [45]. It therefore appears that the long acyl chain of the VLC-GalCers prevented these lipids from mixing ideally with PSM, possibly due to the chain disparity in the hydrophobic part of the bilayer.

3.3. Lateral segregation of VLC-SLs with PSM in multicomponent bilayers

The partial miscibility of the VLC-SLs and PSM and the relatively high melting temperatures suggest that the mixed SLs could separate laterally in a fluid membrane environment consisting of low T_m phospholipids. The propensity of the mixed SLs to form lateral domains was studied with a fluorescence quenching assay, using tPA as a fluorescent marker for ordered domains and 7SLPC as a fluorescence quenching lipid in the fluid phase. We prepared samples composed of POPC (+7SLPC): PSM: 24:0-SL: cholesterol (60:15:15:10, molar ratio) with POPC replacing the 24:0-SL in a PSM reference sample (Fig. 3). As observed in Fig. 3A, the tPA probe was protected from quenching at low temperature in both the 24:0-SM and the 24:0-GalCer containing samples (light and dark grey lines) indicating that ordered domains were formed in the multicomponent membranes. Heating of the bilayers resulted in an increase in the quenching efficiency in the temperature interval (20–47 °C) of domain dissociation. The domain dissociation temperatures were significantly higher in the 24:0-SM or 24:0-GalCer containing samples than in the reference sample with the same amount of PSM without 24:0-SL (black line), showing that both SLs (PSM and 24:0-SL) contributed to the formation and stability of the ordered domains detected by tPA. When 24:0-GlcCer was included in the bilayer, the results obtained were essentially similar to those obtained with 24:0-GalCer and are not shown for the sake of clarity. We noticed from our calorimetric data that the shapes of the 24:0-GalCer and the 24:0-GlcCer thermograms were more identical when the two lipids were mixed with PSM. This was also evident from the more complex lipid mixtures where the GalCer and GlcCer usually showed similar behavior, and is what we also experience from studies on the corresponding 16:0-GSLs in complex mixtures containing PSM [27]. However, the 24:0-GalCer domains were consistently slightly (about 5 °C) more thermostable than the 24:0-GlcCer domains. A similar finding has been reported in comparative studies on galacto- and glucoglycerolipids, which suggest

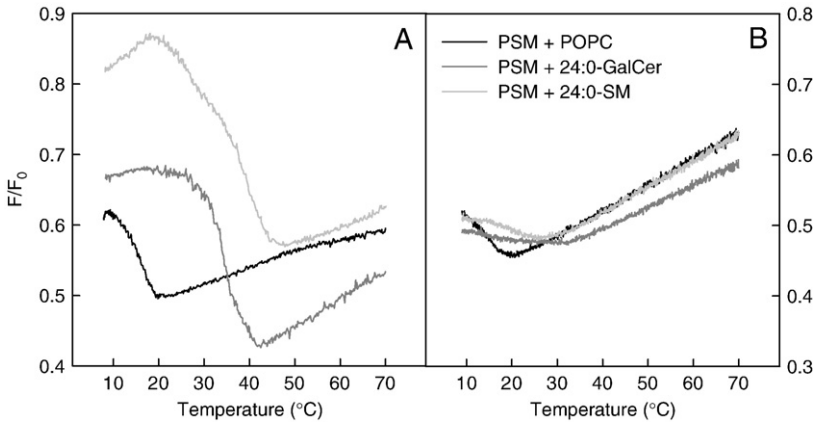

Fig. 3. The presence and thermostability of ordered domains in multicomponent bilayers containing a 24:0-SL and PSM was evaluated with a fluorescence quenching assay. The bilayers were composed of 60 mol% POPC (+7SLPC in *F* samples), 10 mol% cholesterol and 30 mol% of the indicated lipids mixed 1:1, and probed with 1 mol% tPA (panel A) or CTL (panel B). The lipid concentration was 50 μM and the scan rate was 5 °C/min. tPA and CTL were used as markers for ordered and ordered sterol-enriched domains, respectively. A high relative fluorescence intensity value (F/F_0) indicates the coexistence of ordered and disordered domains in the bilayers, and the temperature induced decrease in F/F_0 gives a measure of the stability of the ordered domains. A straight and gradually ascending curve implies that the probe is continuously quenched, either because no ordered domains are present which would shield the probe from quenching, or that the probe is excluded from the ordered domains. Samples containing 30 mol% PSM + 24:0-GlcCer exhibited similar quenching data as those containing 30 mol% PSM + 24:0-GalCer but the tPA curve was shifted to a 5 °C lower temperature (not shown).

that the galactocompounds confer higher stability to membrane phases [57,58]. This seems to result from a different hydrogen bonding pattern of the two glycolipids and a higher hydration of glucose compared to galactose that leads to decreased intermolecular interactions of the glucose containing lipids [59].

The distribution of cholesterol in similar systems was explored with the fluorescent cholesterol analog CTL (Fig. 3B). CTL has been shown to mimic the membrane behavior of cholesterol very well compared to many other cholesterol analogs [40,60–62] and the quenching of CTL by 7SLPC can be used to detect the sterol distribution in membranes with coexisting ordered and disordered domains [45]. The quenching efficiency of CTL was high at low temperature in the 24:0-SL containing bilayers showing that the sterol was predominantly excluded from the mixed SL domains. However, the CTL probe still sensed the domain dissociation in both samples (observed as kinks in the traces at 26–32 °C) indicating that the sterol was at least to some extent associated with the ordered PSM/24:0-SL domains. We may confidently conclude that both SLs present in the mixtures (and not only PSM) associated with the sterol since the release of CTL from the ordered domains was shifted to a higher temperature when a 24:0-SL was included in the bilayer in addition to PSM (light and dark grey line compared to black line). However, from the tPA quenching data in Fig. 3A it seemed that the bilayer containing PSM + 24:0-SM experienced a two-step melting process, possibly suggesting the dissociation of two compositionally different types of ordered domains in the system, e.g. sterol-enriched and sterol-poor domains. In a previous study we showed that PSM and 16:0-GalCer form ordered sterol-enriched domains in a fluid POPC environment as detected by the same fluorescence quenching technique [27]. In the present study we observed that the highly stable ordered domains formed by 24:0-GalCer and PSM at similar conditions (Fig. 3A), were not as prone to include sterols as the 16:0-GalCer/PSM domains (Fig. 3B and [27]). The different tendency of cholesterol to co-localize with GalCers of different chain lengths is in line with a recent TOF-SIMS study on the lipid distribution in rat cerebellum, where the authors identified C18-GalCer in cholesterol-rich regions separate from C24-GalCer enriched regions that were poor in cholesterol [63]. We observed no difference in the propensity to co-localize with cholesterol between the 24:0-GlcCer and 24:0-GalCer, which was slightly surprising since we have previously found that 16:0-GlcCer is more prone to interact with cholesterol than 16:0-GalCer [27].

The stability of the ordered domains was markedly reduced when the 24:0-SLs were replaced by the corresponding unsaturated ones (Fig. 4), i.e. in bilayers composed of POPC (+7SLPC): PSM: 24:1-SL: cholesterol (60:15:15:10, molar ratio). tPA detected domain dissociation temperatures below 25 °C in all samples (Fig. 4A). Incorporation

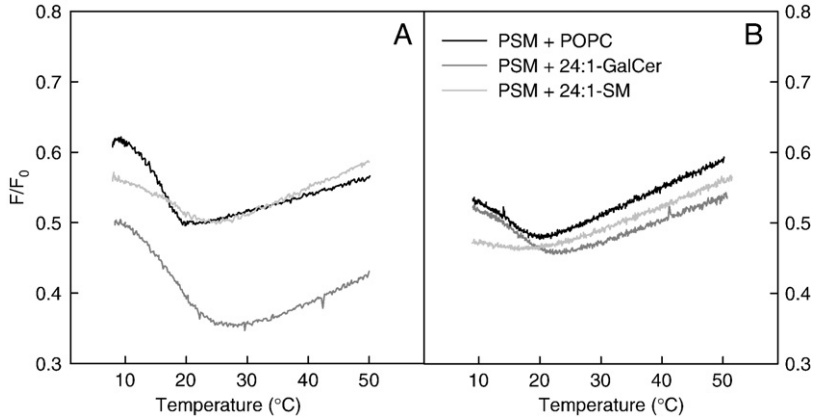

Fig. 4. The presence and thermostability of ordered domains in multicomponent bilayers containing a 24:1-SL and PSM was evaluated with a fluorescence quenching assay. The bilayers were composed of 60 mol% POPC (+7SLPC in *F* samples), 10 mol% cholesterol and 30 mol% of the indicated lipids mixed 1:1, and probed with 1 mol% tPA (panel A) or CTL (panel B). See legend to Fig. 3 for more details. The quenching data of samples containing 30 mol% PSM + 24:1-GlcCer was equivalent to that containing 30 mol% PSM + 24:1-GalCer (not shown).

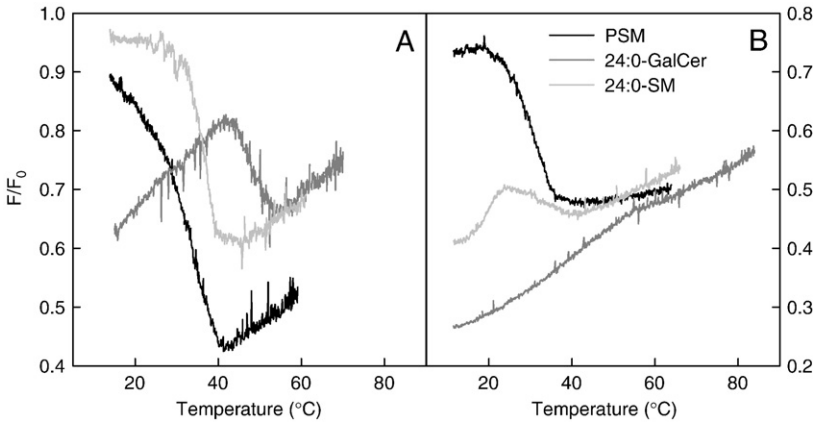

Fig. 5. The presence and thermostability of ordered domains in multicomponent bilayers containing a 24:0-SL was evaluated with a fluorescence quenching assay. The bilayers were composed of 60 mol% POPC (+7SLPC in *F* samples), 10 mol% cholesterol and 30 mol% of the SLs indicated in the figure, and probed with 1 mol% tPA (panel A) or CTL (panel B). See legend to Fig. 3 for more details. Samples containing 30 mol% 24:0-GlcCer exhibited similar quenching data as those containing 30 mol% 24:0-GalCer but was shifted to a 5 °C lower temperature (not shown).

of 24:1-GalCer (or 24:1-GlcCer, data not shown) into the membranes in addition to PSM shifted the domain dissociation to a slightly higher temperature (comparing the dark grey line with the black line), whereas addition of 24:1-SM seemed to make tPA more susceptible to quenching (a lower $\Delta F/F_0$ value for the light grey line compared to the black line). A similar pattern was observed with CTL, i.e. 24:1-GalCer stabilized the PSM/sterol domains slightly while inclusion of 24:1-SM increased the quenching efficiency of CTL in the 24:1-SM/PSM sample compared to the PSM sample (Fig. 4B). The effect of 24:1-SM on the PSM rich domains in multicomponent membranes differed from that of the other VLC-SLs studied. Whereas the unsaturated chain drove 24:1-GalCer mostly towards the disordered POPC rich phase to leave the PSM/cholesterol domains relatively unaffected, it seemed that 24:1-SM mixed with and perturbed the packing of the ordered PSM rich domains (Fig. 4).

To summarize the results in Figs. 3 and 4, the combined data recorded with tPA and CTL indicates that ordered PSM/24:0-SL domains were indeed formed but they did not accommodate sterol, whereas the PSM/24:1-SL mixtures did not form ordered domains to the same extent and were therefore not able to shield much of the sterol from the quencher.

3.4. Lateral segregation of VLC-SLs in multicomponent bilayers

Finally, we analyzed the potential formation of VLC-SL microdomains in a POPC/cholesterol bilayer in the absence of PSM to examine if the long acyl chains favored homo-association of the SLs as opposed to preferential co-clustering with SMs. The tendency of the VLC-SLs to cluster together and form ordered, possibly sterol-enriched, domains was explored in bilayers containing 30 mol% VLC-SL. The lipid composition of the samples used in Fig. 5 was POPC (+7SLPC): 24:0-SL: cholesterol (60:30:10, molar ratio), and PSM replaced the 24:0-SL in the PSM reference sample. As observed in Fig. 5A, both 24:0-SM and 24:0-GalCer were able to form ordered domains in the fluid membrane environment as shown by the temperature induced increase in quenching efficiency of tPA. The thermostability of the 24:0-SM domains (light grey line) was similar to that detected for PSM domains (black line), whereas the 24:0-GalCer domains were even more stable (dark grey line). The low starting F/F_0 value of 24:0-GalCer suggests that the 24:0-GalCer rich domains had a very tight lateral packing that did not allow the tPA probe to intercalate between the GalCer molecules until the domain structure was loosened up by the temperature increase, as has previously been observed for 16:0-GalCer rich domains in similar systems [27]. A bilayer containing 30% 24:0-GlcCer as the potential ordered domain forming lipid exhibited tPA quenching data similar to that of the 24:0-GalCer sample, but the domain dissociation was shifted to a temperature about 5 °C lower (not shown).

The PSM domains were enriched in sterols, as evident from Fig. 5B showing the domain dissociation process as experienced by the CTL

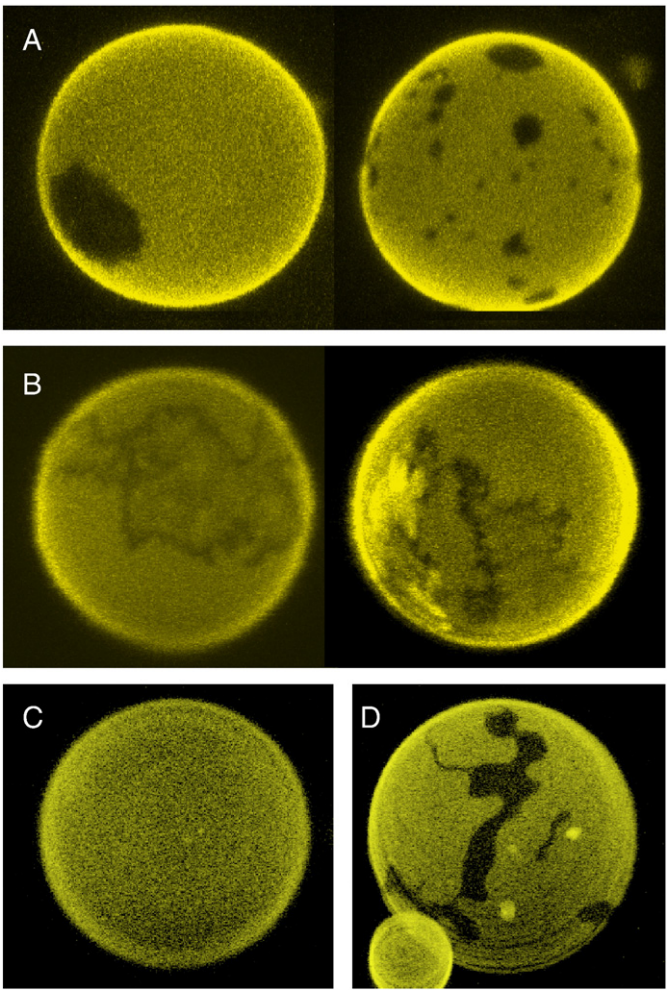

Fig. 6. Confocal fluorescence intensity images of DiIC18 labeled GUVs at 20 °C. The lipid composition of the vesicles was POPC: VLC-SL: cholesterol (60:30:10, molar ratio), where the VLC-SL was A) 24:0-SM, B) 24:0-GalCer, C) 24:1-SM, D) 24:1-GalCer. DiI_{C18} is excluded from ordered phases and the labeled yellow areas correspond to disordered domains.

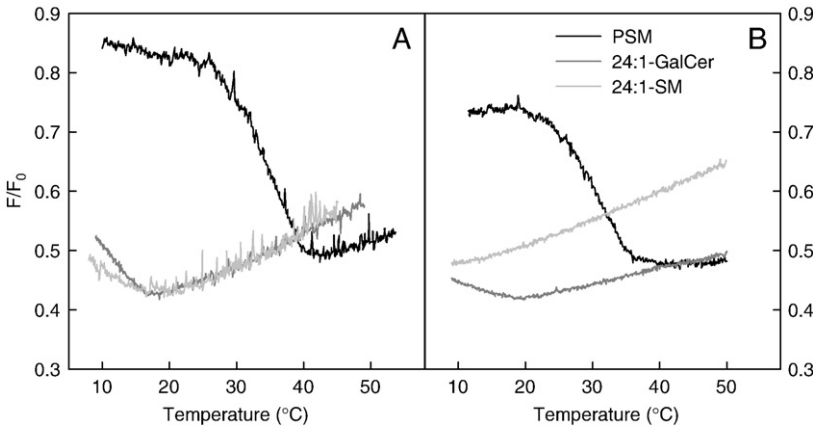

Fig. 7. The potential presence of ordered domains in multicomponent bilayers containing a 24:1-SL was evaluated with a fluorescence quenching assay. The bilayers were composed of 60 mol% POPC (+7SLPC in *F* samples), 10 mol% cholesterol and 30 mol% of the SLs indicated in the figure, and probed with 1 mol% tPA (panel A) or CTL (panel B). See legend to Fig. 3 for more details. The quenching data of samples containing 30 mol% 24:1-GlcCer was equivalent to that containing 30 mol% 24:1-GalCer (not shown).

probe. CTL and tPA detected the melting of the PSM domains in the same temperature interval, in analogy with previous results [27]. From Fig. 5B it is also clear that the 24:0-GalCer domains did not include sterol, since CTL was quenched already at low temperature and the quenching curve was essentially straight over the whole temperature interval studied. The same was observed with 24:0-GlcCer (not shown). The 24:0-SM on the other hand, seemed to accommodate some of the sterol, although the sterol did not partition into the 24:0-SM domains as readily as into the PSM domains (comparing the $\Delta F/F_0$ of the light grey and the black lines). However, the sterol was shielded from quenching up to a higher temperature in bilayers containing 30 mol% 24:0-SM than in bilayers containing 15 mol% PSM + 15 mol% 24:0-SM (Fig. 3B). As was already discussed for 24:0-GalCer in the multicomponent membranes, it appeared that the 24:0 chain also hindered 24:0-SM from interacting with cholesterol, since the sterol inclusion in the ordered domains was smaller in bilayers containing 15% PSM + 15% 24:0-SM (Fig. 3B) or 30% 24:0-SM (Fig. 5B) than in bilayers containing 30% PSM (Fig. 5B). Interestingly, the cooling scans of the samples containing 30% 24:0-GalCer or 24:0-GlcCer were not reversible and the hysteretic behavior seen with DSC in the pure VLC-GSL bilayers was clearly observable also in the more complex mixtures (cooling scans not shown).

The lateral organization of similar lipid mixtures as those studied in Fig. 5 was also studied with confocal fluorescence microscopy. GUVs were prepared of POPC: 24:0-SL: cholesterol (60:30:10, molar ratio) labeled with DiI_{C18} and imaged at 20 °C (Fig. 6). Two distinct phases were observed in the membranes, the yellow labeled areas presumably corresponding to fluid phase since DiI_{C18} has previously been shown to be excluded from ordered phases in similar lipid mixtures [42,64]. The 24:0-SM containing GUVs (Fig. 6A) displayed non-fluorescent domains that were fairly circular in shape compared to the irregularly shaped domains observed in the 24:0-GalCer containing bilayer (Fig. 6B). This is indicative of a higher inclusion of sterols in the 24:0-SM rich domains that makes them more fluid-like at 20 °C than the 24:0-GalCer domains, which most likely were in the gel phase. This is in line with the CTL fluorescence quenching data shown in Fig. 5B. However, the ordered domains in GUVs containing PSM instead of 24:0-SL were even more circular and mobile on the vesicle surface, and thus displayed typical liquid-ordered phase behavior (not shown).

When the GUVs were prepared to contain 30 mol% 24:1-SL instead of 24:0-SL, we observed no phase separation in 24:1-SM containing vesicles (Fig. 6C), whereas two phases were seen in those containing 24:1-GalCer (Fig. 6D). The non-fluorescent areas in the latter displayed a domain morphology that was intermediate between that of the samples containing 24:0-SM or 24:0-GalCer (Fig. 6A and B, respectively). These striped domains were hardly discernible in some individual vesicles (not shown). A plausible explanation for the ambiguity in the 24:1-GalCer sample could be that the temperature at which the GUV images were taken was very close to the melting temperature of the 24:1-GalCer rich domains. This was indeed evident from the fluorescence quenching data on similar lipid mixtures. The small vesicles used in Fig. 7 were prepared of POPC (+7SLPC): 24:1-SL: cholesterol (60:30:10, molar ratio) and thus, the only compositional difference (apart from a different probe) from Fig. 6C and D was the absence of the quencher lipid in the GUVs. According to fluorescence quenching of tPA (Fig. 7A), ordered domains were present in the 24:1-GalCer containing system up to temperatures around 20 °C (dark grey line). These were thus considerably less thermostable than the 24:0-GalCer or PSM domains formed in corresponding systems (Figs. 5A and 7A). The results were also confirmed with DSC experiments on similar lipid mixtures (POPC: 24:1-GalCer: cholesterol, 60:30:10, molar ratio) which displayed a broad endothermic peak between 0 and 20 °C but no detectable transitions above 20 °C (not shown). This miscibility temperature (~20 °C) is in reasonable agreement with that observed in a previous study on POPC/GalCer/cholesterol mixtures where a natural mixture of bovine GalCers was used [29]. Lin et al. reported that the transition from liquid + liquid phase coexistence to only one fluid phase occurs at a cholesterol concentration of 17.5 mol% at room temperature [29]. We observed this to occur at 10 mol% cholesterol in our system where acyl chain specific 24:1-GalCers were used. CTL quenching showed that the 24:1-GalCer enriched domains included some sterols up to about 20 °C (Fig. 7B) which could explain their fluid-like appearance in the GUV membranes. 24:1-SM was less prone to form ordered domains, as evident from both tPA and CTL quenching (Fig. 7A, B) and also consistent with the GUV figures.

4. Conclusions

We can conclude from this study that the molecular structure of the VLC-GSLs studied gives them complex thermotropic behavior in bilayers which affects the way these lipids interact with other membrane components, such as cholesterol, and the lateral structures that they form. Lipids with high T_m are usually considered good candidates for participation in ordered domain formation in membranes. However, the DPH anisotropy data showed that the 24:1-GSLs, which have high melting temperatures, displayed a lower membrane order within the physiological temperature range than for instance 24:0-SM, which had a substantially lower T_m. The double bond at position C15 in the acyl chain of the 24:1-SLs occurs close to the bilayer midplane. At this position it is expected to disturb the chain packing less than a double bond located at C9, which is common in

naturally occurring glycerophospholipids [19]. The double bond at C15 still seemed to largely interfere with the lipid chain order in the gel phase according to the DPH results. This may also be noted from the decrease in T_m of about 20 °C for all 24:1-SLs as compared to the corresponding 24:0-SLs. The ability to pack tightly with ordered and extended acyl chains is another necessity for membrane lipids to be able to build up ordered domains in membranes and thus the 24:1-GSLs appeared less likely to participate in ordered domain formation.

The 24:0-SLs studied formed highly stable domains in fluid phospholipid membranes, both when present as the only SL in the bilayer and together with PSM. However, cholesterol partitioned poorly into the SL domains when 24:0-SLs were included. We speculate that the sterol partitioning was hindered by a very high lateral packing density mediated by the very long saturated acyl chains. There was however an effect of the polar head group, since 24:0-SM was better able to accommodate sterol than the GSLs. The much higher partitioning of sterol into ordered domains containing 16:0-GSLs [27] than 24:0-GSLs (this study) again indicates the importance of the acyl chain which may be explained by effects of the bilayer thickness or intramolecular acyl chain asymmetry.

The GalCers nicely exemplify the effect of unsaturated vs saturated very long acyl chains on domain formation by the GSLs. The long unsaturated chain drove 24:1-GalCer more towards the disordered POPC rich phase than to the PSM rich ordered phase in the complex bilayers, whereas the long saturated chain allowed tight interaction of 24:0-GalCer with PSM. This may furthermore explain the slightly higher enrichment of sterols into the ordered domains in bilayers containing PSM and 24:1-GalCer than in bilayers containing PSM and 24:0-GalCer. The sterol was presumably hindered by the higher packing density of the PSM/24:0-GalCer domains compared to the almost pure PSM domains that were present with 24:1-GalCer. Based on this observation, it was also expected that the sterol would be excluded from the ordered 24:0-GalCer domains in the absence of PSM, as it was according to CTL quenching and which was also indicated by the shape of the 24:0-GalCer rich domains seen in the GUVs.

The most disordered lipid used in this study, 24:1-SM, appeared to mix reasonably well with PSM and was even able to hinder the formation of ordered PSM/cholesterol domains. The DSC analysis of the binary 24:1-SM/PSM mixture showed it was the only one in this study that melted below physiological temperature. 24:1-SM was thus a more “disordered” lipid than 24:1-GalCer and 24:1-GlcCer. This finding was in line with a recent study on the lipid composition of membrane microdomains in THP-1 macrophages [65]. The authors found 24:1-GlcCer to accompany 24:0- and 16:0-GlcCer in the detergent resistant fractions of the cell membranes, whereas 24:1-SM was mainly distributed to the soluble domains in contrast to 24:0- and 16:0-SM [65]. Considering the low T_m of 24:1-SM and the disordering effect of the lipid on PSM domains it was expected to also find the 24:1-SM unable to form ordered domains in the absence of other domain building lipids in the complex membranes.

Sphingolipids containing very long acyl chains are abundant in certain specialized tissues and are minor components of plasma membranes in most mammalian cells. There is evidence of cellular processes in which sphingolipids specifically containing long acyl chains are required, and the function is thought to be mediated through sphingolipid-rich membrane domains [5,6]. This study was conducted to explore the physical membrane properties of various naturally relevant SLs containing very long acyl chains to get deeper insight into the molecular features that influence the lateral distribution of different SLs and cholesterol between functional SL-enriched domains in biological membranes. Based on the results of the present study, it appears possible that the increased levels of VLC-SLs that occur at some physiological and pathological conditions may have a specific function. It is also evident that the specific molecular structure of the VLC-SL and not only the very long acyl chain per se is of importance for this function. Depending on which VLC-SL is present they will influence the function of membrane domain mediated cellular events, either through effects on the sterol distribution between ordered and disordered domains or through differences in the biophysical properties of the VLC-SL-enriched domains as compared to domains enriched in short chain SLs.

Acknowledgements

The authors want to thank Stina Maunula for performing some initial experiments. The Packaléns Mindefond Foundation is acknowledged for travel grants. This study was supported by the Academy of Finland, the Sigrid Juselius Foundation, Forskningsrådet for Natur og Univers (FNU, Denmark), the Danish National Research Foundation, Svenska Kulturfonden, the Oskar Öflund Foundation, the K. Albin Johansson Foundation, the Magnus Ehrnrooth Foundation, Kommersrådet Otto A. Malms donationsfond and Medicinska Understödsföreningen Liv och Hälsa. The work of Y.J.E. Björkqvist was supported by the National Graduate School in Informational and Structural Biology at Åbo Akademi University.

References

[1] N. Taieb, N. Yahi, J. Fantini, Rafts and related glycosphingolipid-enriched microdomains in the intestinal epithelium: bacterial targets linked to nutrient absorption, Adv. Drug Deliv. Rev. 56 (2004) 779–794.
[2] K. Kasahara, Y. Sanai, Functional roles of glycosphingolipids in signal transduction via lipid rafts, Glycoconj. J. 17 (2000) 153–162.
[3] S. Hakomori, Glycosynapses: microdomains controlling carbohydrate-dependent cell adhesion and signaling, An. Acad. Bras. Cienc. 76 (2004) 553–572.
[4] A.E. Leonard, S.L. Pereira, H. Sprecher, Y.S. Huang, Elongation of long-chain fatty acids, Prog. Lipid Res. 43 (2004) 36–54.
[5] B. Gaigg, A. Toulmay, R. Schneiter, Very long-chain fatty acid-containing lipids rather than sphingolipids per se are required for raft association and stable surface transport of newly synthesized plasma membrane ATPase in yeast, J. Biol. Chem. 281 (2006) 34135–34145.
[6] K. Iwabuchi, A. Prinetti, S. Sonnino, L. Mauri, T. Kobayashi, K. Ishii, N. Kaga, K. Murayama, H. Kurihara, H. Nakayama, F. Yoshizaki, K. Takamori, H. Ogawa, I. Nagaoka, Involvement of very long fatty acid-containing lactosylceramide in lactosylceramide-mediated superoxide generation and migration in neutrophils, Glycoconj. J. 25 (2008) 357–374.
[7] S.J. Crook, J.M. Boggs, A.I. Vistnes, K.M. Koshy, Factors affecting surface expression of glycolipids: influence of lipid environment and ceramide composition on antibody recognition of cerebroside sulfate in liposomes, Biochemistry 25 (1986) 7488–7494.
[8] Y. Tagawa, W. Laroy, L. Nimrichter, S.E. Fromholt, A.B. Moser, H.W. Moser, R.L. Schnaar, Anti-ganglioside antibodies bind with enhanced affinity to gangliosides containing very long chain fatty acids, Neurochem. Res. 27 (2002) 847–855.
[9] D.H. Jones, C.A. Lingwood, K.R. Barber, C.W. Grant, Globoside as a membrane receptor: a consideration of oligosaccharide communication with the hydrophobic domain, Biochemistry 36 (1997) 8539–8547.
[10] M.R. Morrow, D.M. Singh, C.W. Grant, Glycosphingolipid headgroup orientation in fluid phospholipid/cholesterol membranes: similarity for a range of glycolipid fatty acids, Biophys. J. 69 (1995) 955–964.
[11] K.S. Hamilton, K. Briere, H.C. Jarrell, C.W. Grant, Acyl chain length effects related to glycosphingolipid crypticity in phospholipid membranes: probed by 2H-NMR, Biochim. Biophys. Acta 1190 (1994) 367–375.
[12] X.M. Li, J.M. Smaby, M.M. Momsen, H.L. Brockman, R.E. Brown, Sphingomyelin interfacial behavior: the impact of changing acyl chain composition, Biophys. J. 78 (2000) 1921–1931.
[13] J.M. Smaby, V.S. Kulkarni, M. Momsen, R.E. Brown, The interfacial elastic packing interactions of galactosylceramides, sphingomyelins, and phosphatidylcholines, Biophys. J. 70 (1996) 868–877.
[14] X. Zhai, X.M. Li, M.M. Momsen, H.L. Brockman, R.E. Brown, Lactosylceramide: lateral interactions with cholesterol, Biophys. J. 91 (2006) 2490–2500.
[15] I.W. Levin, T.E. Thompson, Y. Barenholz, C. Huang, Two types of hydrocarbon chain interdigitation in sphingomyelin bilayers, Biochemistry 24 (1985) 6282–6286.
[16] P.R. Maulik, D. Atkinson, G.G. Shipley, X-ray scattering of vesicles of N-acyl sphingomyelins. Determination of bilayer thickness, Biophys. J. 50 (1986) 1071–1077.
[17] I.E. Mehlhorn, E. Florio, K.R. Barber, C. Lordo, C.W. Grant, Evidence that transbilayer interdigitation of glycosphingolipid long chain fatty acids may be a general phenomenon, Biochim. Biophys. Acta 939 (1988) 151–159.
[18] J.M. Boggs, K.M. Koshy, Do the long fatty acid chains of sphingolipids interdigitate across the center of a bilayer of shorter chain symmetric phospholipids? Biochim. Biophys. Acta 1189 (1994) 233–241.
[19] P.S. Niemela, M.T. Hyvonen, I. Vattulainen, Influence of chain length and unsaturation on sphingomyelin bilayers, Biophys. J. 90 (2006) 851–863.
[20] W. Curatolo, F.B. Jungalwala, Phase behavior of galactocerebrosides from bovine brain, Biochemistry 24 (1985) 6608–6613.

[21] V.S. Kulkarni, W.H. Anderson, R.E. Brown, Bilayer nanotubes and helical ribbons formed by hydrated galactosylceramides: acyl chain and headgroup effects, Biophys. J. 69 (1995) 1976–1986.
[22] R.A. Reed, G.G. Shipley, Structure and metastability of N-lignocerylgalactosylsphingosine (cerebroside) bilayers, Biochim. Biophys. Acta 896 (1987) 153–164.
[23] E. Freire, D. Bach, M. Correa-Freire, I. Miller, Y. Barenholz, Calorimetric investigation of the complex phase behavior of glucocerebroside dispersions, Biochemistry 19 (1980) 3662–3665.
[24] M. Gardam, J.R. Silvius, Intermixing of dipalmitoylphosphatidylcholine with phospho- and sphingolipids bearing highly asymmetric hydrocarbon chains, Biochim. Biophys. Acta 980 (1989) 319–325.
[25] M.R. Morrow, D. Singh, D. Lu, C.W. Grant, Glycosphingolipid phase behaviour in unsaturated phosphatidylcholine bilayers: a 2H-NMR study, Biochim. Biophys. Acta 1106 (1992) 85–93.
[26] B. Maggio, M.L. Fanani, C.M. Rosetti, N. Wilke, Biophysics of sphingolipids II. Glycosphingolipids: an assortment of multiple structural information transducers at the membrane surface, Biochim. Biophys. Acta 1758 (2006) 1922–1944.
[27] S. Maunula, Y.J. Bjorkqvist, J.P. Slotte, B. Ramstedt, Differences in the domain forming properties of N-palmitoylated neutral glycosphingolipids in bilayer membranes, Biochim. Biophys. Acta 1768 (2007) 336–345.
[28] T.Y. Wang, J.R. Silvius, Sphingolipid partitioning into ordered domains in cholesterol-free and cholesterol-containing lipid bilayers, Biophys. J. 84 (2003) 367–378.
[29] W.C. Lin, C.D. Blanchette, M.L. Longo, Fluid-phase chain unsaturation controlling domain microstructure and phase in ternary lipid bilayers containing GalCer and cholesterol, Biophys. J. 92 (2007) 2831–2841.
[30] D.N. Arvanitis, W. Min, Y. Gong, Y.M. Heng, J.M. Boggs, Two types of detergent-insoluble, glycosphingolipid/cholesterol-rich membrane domains from isolated myelin, J. Neurochem. 94 (2005) 1696–1710.
[31] B. Brugger, C. Graham, I. Leibrecht, E. Mombelli, A. Jen, F. Wieland, R. Morris, The membrane domains occupied by glycosylphosphatidylinositol-anchored prion protein and Thy-1 differ in lipid composition, J. Biol. Chem. 279 (2004) 7530–7536.
[32] K. Iwabuchi, K. Handa, S. Hakomori, Separation of "glycosphingolipid signaling domain" from caveolin-containing membrane fraction in mouse melanoma B16 cells and its role in cell adhesion coupled with signaling, J. Biol. Chem. 273 (1998) 33766–33773.
[33] J.W. Hinrichs, K. Klappe, R.M. van, J.W. Kok, Drug resistance-associated changes in sphingolipids and ABC transporters occur in different regions of membrane domains, J. Lipid Res. 46 (2005) 2367–2376.
[34] R. Cohen, Y. Barenholz, S. Gatt, A. Dagan, Preparation and characterization of well defined D-*erythro* sphingomyelins, Chem. Phys. Lipids 35 (1984) 371–384.
[35] Y.J. Bjorkqvist, S. Nybond, T.K. Nyholm, J.P. Slotte, B. Ramstedt, N-palmitoylsulfatide participates in lateral domain formation in complex lipid bilayers, Biochim. Biophys. Acta 1778 (2008) 954–962.
[36] S. Nybond, Y.J. Bjorkqvist, B. Ramstedt, J.P. Slotte, Acyl chain length affects ceramide action on sterol/sphingomyelin-rich domains, Biochim Biophys Acta 1718 (2005) 61–66.
[37] B. Ramstedt, J.P. Slotte, Interaction of cholesterol with sphingomyelins and acyl-chain-matched phosphatidylcholines: a comparative study of the effect of the chain length, Biophys. J. 76 (1999) 908–915.
[38] B. Ramstedt, J.P. Slotte, Comparison of the biophysical properties of racemic and D-erythro-N-acyl sphingomyelins, Biophys. J. 77 (1999) 1498–1506.
[39] G. Szolderits, G. Daum, F. Paltauf, A. Hermetter, Protein-catalyzed transport of ether phospholipids, Biochim. Biophys. Acta 1063 (1991) 197–202.
[40] R.T. Fischer, F.A. Stephenson, A. Shafiee, F. Schroeder, delta 5,7,9(11)-Cholestatrien-3 beta-ol: a fluorescent cholesterol analogue, Chem. Phys. Lipids 36 (1984) 1–14.
[41] L.A. Sklar, B.S. Hudson, R.D. Simoni, Conjugated polyene fatty acids as fluorescent probes: synthetic phospholipid membrane studies, Biochemistry 16 (1977) 819–828.
[42] M. Fidorra, L. Duelund, C. Leidy, A.C. Simonsen, L.A. Bagatolli, Absence of fluid-ordered/fluid-disordered phase coexistence in ceramide/POPC mixtures containing cholesterol, Biophys. J. 90 (2006) 4437–4451.
[43] M.I. Angelova, S. Soleau, P. Meleard, J.F. Faucon, P. Bothorel, Preparation of giant vesicles by external AC fields. Kinetics and application, Prog. Colloid Polym. Sci. 89 (1992) 127–131.
[44] S.M. Alanko, K.K. Halling, S. Maunula, J.P. Slotte, B. Ramstedt, Displacement of sterols from sterol/sphingomyelin domains in fluid bilayer membranes by competing molecules, Biochim. Biophys. Acta 1715 (2005) 111–121.
[45] Y.J.E. Björkqvist, T.K.M. Nyholm, J.P. Slotte, B. Ramstedt, Domain formation and stability in complex lipid bilayers as reported by cholestatrienol, Biophys. J. 88 (2005) 4054–4063.
[46] P.R. Maulik, G.G. Shipley, X-ray diffraction and calorimetric study of N-lignoceryl sphingomyelin membranes, Biophys. J. 69 (1995) 1909–1916.
[47] V.S. Kulkarni, R.E. Brown, Thermotropic behavior of galactosylceramides with cis-monoenoic fatty acyl chains, Biochim. Biophys. Acta 1372 (1998) 347–358.
[48] P.K. Sripada, P.R. Maulik, J.A. Hamilton, G.G. Shipley, Partial synthesis and properties of a series of N-acyl sphingomyelins, J. Lipid Res. 28 (1987) 710–718.
[49] T.J. McIntosh, S.A. Simon, D. Needham, C.H. Huang, Structure and cohesive properties of sphingomyelin/cholesterol bilayers, Biochemistry 31 (1992) 2012–2020.
[50] K. Saxena, R.I. Duclos, P. Zimmermann, R.R. Schmidt, G.G. Shipley, Structure and properties of totally synthetic galacto- and gluco-cerebrosides, J. Lipid Res. 40 (1999) 839–849.
[51] R.N. Lewis, D.A. Mannock, R.N. McElhaney, Differential scanning calorimetry in the study of lipid phase transitions in model and biological membranes: practical considerations, Methods Mol. Biol. 400 (2007) 171–195.
[52] P.R. Maulik, G.G. Shipley, N-palmitoyl sphingomyelin bilayers: structure and interactions with cholesterol and dipalmitoylphosphatidylcholine, Biochemistry 35 (1996) 8025–8034.
[53] T.K.M. Nyholm, M. Nylund, J.P. Slotte, A calorimetric study of binary mixtures of dihydrosphingomyelin and sterols, sphingomyelin, or phosphatidylcholine, Biophys. J. 84 (2003) 3138–3146.
[54] K. Florine-Casteel, G.W. Feigenson, On the use of partition coefficients to characterize the distribution of fluorescent membrane probes between coexisting gel and fluid lipid phase: an analysis of the partition behavior of 1,6-diphenyl-1,3,5-hexatriene, Biochim. Biophys. Acta 941 (1988) 102–106.
[55] T.P. McMullen, R.N. McElhaney, New aspects of the interaction of cholesterol with dipalmitoylphosphatidylcholine bilayers as revealed by high-sensitivity differential scanning calorimetry, Biochim. Biophys. Acta 1234 (1995) 90–98.
[56] Y. Barenholz, E. Freire, T.E. Thompson, M.C. Correa-Freire, D. Bach, I.R. Miller, Thermotropic behavior of aqeuous dispersions of glucosylceramide-dipalmitoylphosphatidylcholine mixtures, Biochemistry 22 (1983) 3497–3501.
[57] H.J. Hinz, H. Kuttenreich, R. Meyer, M. Renner, R. Frund, R. Koynova, A.I. Boyanov, B.G. Tenchov, Stereochemistry and size of sugar head groups determine structure and phase behavior of glycolipid membranes: densitometric, calorimetric, and X-ray studies, Biochemistry 30 (1991) 5125–5138.
[58] D.A. Mannock, P.E. Harper, S.M. Gruner, R.N. McElhaney, The physical properties of glycosyl diacylglycerols. Calorimetric, X-ray diffraction and Fourier transform spectroscopic studies of a homologous series of 1,2-di-O-acyl-3-O-(beta-D-galactopyranosyl)-sn-glycerols, Chem. Phys. Lipids 111 (2001) 139–161.
[59] T. Rog, I. Vattulainen, A. Bunker, M. Karttunen, Glycolipid membranes through atomistic simulations: effect of glucose and galactose head groups on lipid bilayer properties, J. Phys. Chem. B 111 (2007) 10146–10154.
[60] P.A. Hyslop, B. Morel, R.D. Sauerheber, Organization and interaction of cholesterol and phosphatidylcholine in model bilayer membranes, Biochemistry 29 (1990) 1025–1038.
[61] H.A. Scheidt, P. Muller, A. Herrmann, D. Huster, The potential of fluorescent and spin-labeled steroid analogs to mimic natural cholesterol, J. Biol. Chem. 278 (2003) 45563–45569.
[62] F. Schroeder, G. Nemecz, E. Gratton, Y. Barenholz, T.E. Thompson, Fluorescence properties of cholestatrienol in phosphatidylcholine bilayer vesicles, Biophys. Chem. 32 (1988) 57–72.
[63] K. Borner, H. Nygren, B. Hagenhoff, P. Malmberg, E. Tallarek, J.E. Mansson, Distribution of cholesterol and galactosylceramide in rat cerebellar white matter, Biochim. Biophys. Acta 1761 (2006) 335–344.
[64] M. Fidorra, T. Heimburg, L.A. Bagatolli, Headgroup influence on membrane shapes and lateral membrane structure of POPC/ceramides and POPC/cerebrosides mixtures, Biophys J. Volume 90 (Abstracts issue, January 2006).
[65] L.K. Hein, S. Duplock, J.J. Hopwood, M. Fuller, Lipid composition of microdomains is altered in a cell model of Gaucher disease, J. Lipid Res. 49 (2008) 1725–1734.